NASA TECHNICAL NOTE

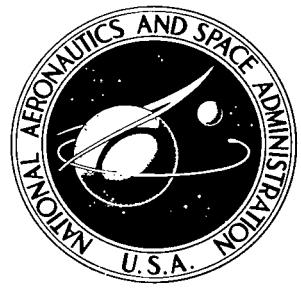

NASA TN D-5388

ANALYSIS OF DYNAMIC PERFORMANCE LIMITATIONS OF FAST RESPONSE (150 TO 200 Hz) ELECTROHYDRAULIC SERVOS

by John R. Zeller

Lewis Research Center

Cleveland, Ohio

NATIONAL AERONAUTICS AND SPACE ADMINISTRATION • WASHINGTON, D. C. • AUGUST 1969

ANALYSIS OF DYNAMIC PERFORMANCE LIMITATIONS OF FAST RESPONSE (150 TO 200 Hz) ELECTROHYDRAULIC SERVOS

By John R. Zeller

Lewis Research Center
Cleveland, Ohio

NATIONAL AERONAUTICS AND SPACE ADMINISTRATION

For sale by the Clearinghouse for Federal Scientific and Technical Information
Springfield, Virginia 22151 – CFSTI price $3.00

ABSTRACT

Fast response (150 to 200 Hz) electrohydraulic valve-controlled piston servo systems are used as research tools in experimental dynamics and controls studies. The components within these systems must operate at their limits of capability to achieve these high rates of response. A detailed nonlinear analytical model of these systems has been formulated. The accuracy of this model has been verified by comparing model dynamic performance against actual experimental data for a specific application. The analysis has led to a new generalized design criterion which in specific applications assists in determining a maximum region of dynamic performance capability.

ANALYSIS OF DYNAMIC PERFORMANCE LIMITATIONS OF FAST RESPONSE (150 TO 200 Hz) ELECTROHYDRAULIC SERVOS

by John R. Zeller

Lewis Research Center

SUMMARY

Activities in the area of advanced propulsion system dynamics and controls research have dictated a need for fast response (150 to 200 Hz) servo actuation systems. The type of equipment normally selected for these applications is the electrohydraulic servovalve and piston-in-cylinder actuator arrangement. In oscillating various propulsion system elements at finite amplitudes and at these high rates (150 to 200 Hz), the system components must operate at the limits of their capability. Thus, component nonlinearities, often neglected in lower response applications, must be considered in determining the dynamic performance capabilities of these systems.

A detailed nonlinear analytical model of these systems is presented. The accuracy of the model is verified by comparing model dynamic performance against actual experimental data for a specific high frequency application. Component performance evaluation made possible with this nonlinear dynamic model resulted in a new design criterion which assists in the selection of system components. This new criterion when combined with existing limit criteria will determine a maximum region of dynamic performance capability for the fast response systems.

INTRODUCTION

Research activities in the areas of advanced propulsion systems have dictated a significant need for high performance, fast response (150 to 200 Hz) servo systems. This need is twofold: first, as disturbance devices for studying the high frequency dynamics of propulsion systems and components; and, second, as a control loop element for complex systems.

The type of equipment normally selected to provide this fast response control capability is the two-stage electrohydraulic servovalve and piston-in-cylinder actuator arrangement. Its basic closed loop configuration is shown in figure 1. The equipment is

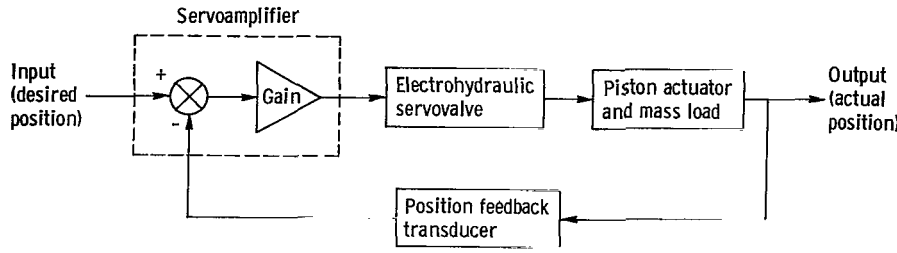

Figure 1. - Basic closed-loop configuration of electrohydraulic servo system.

well suited to this application for several reasons. First, it has the inherent capability of modulating large amounts of energy at the desired high frequency rates. Second, most propulsion system manipulated variables can be arranged in a configuration that adapts well to the linear motion of piston-in-cylinder actuators. Finally, the electrical input nature of the system makes it suitable for accepting well defined input waveforms, thus greatly simplifying the subsequent task of interpreting research performance data.

In many applications employing this control system configuration, the natural hydraulic resonant frequency of the actuator and load combination will limit the range of dynamic performance (ref. 1). In this report, the systems which are to be manipulated at these high rates of response (150 to 200 Hz), however, involve relatively small mass loads. Thus, by hydraulically close-coupling the servovalve and piston actuator to minimize the entrapped volume of hydraulic fluid, the hydraulic spring/load mass resonant frequency can be made to occur well beyond the dynamic performance range of interest.

Elimination of this natural performance limitation puts the close-coupled, low mass electrohydraulic servosystems into a somewhat specialized category. The dynamic performance capabilities of the higher frequency systems now become quite dependent upon certain physical limits of the components. The magnitude and frequency of sinusoidal output performance will be bounded as a function of certain of these limitations. The region within this boundary will be the maximum region of dynamic performance capability.

This report evaluates the effect each component limitation has in determining this boundary. It is intended that the presentation will be detailed enough to demonstrate the value of a nonlinear analysis in evaluating systems with high performance requirements. The analysis also will attempt to establish general design criteria based upon those component limitations found to be significant.

ANALYTICAL DESCRIPTION OF COMPONENTS

Load and Piston Actuator Force Balance

For the category of systems under consideration, the load being actuated by a double-ended cylinder is assumed to have negligible friction and spring (position-dependent) types of loading. Using the notation of figure 2, the following equation results:

$$p_p A_p = M\ddot{x}_o + F_o \tag{1}$$

where

$$p_p = p_1 - p_2 \tag{2}$$

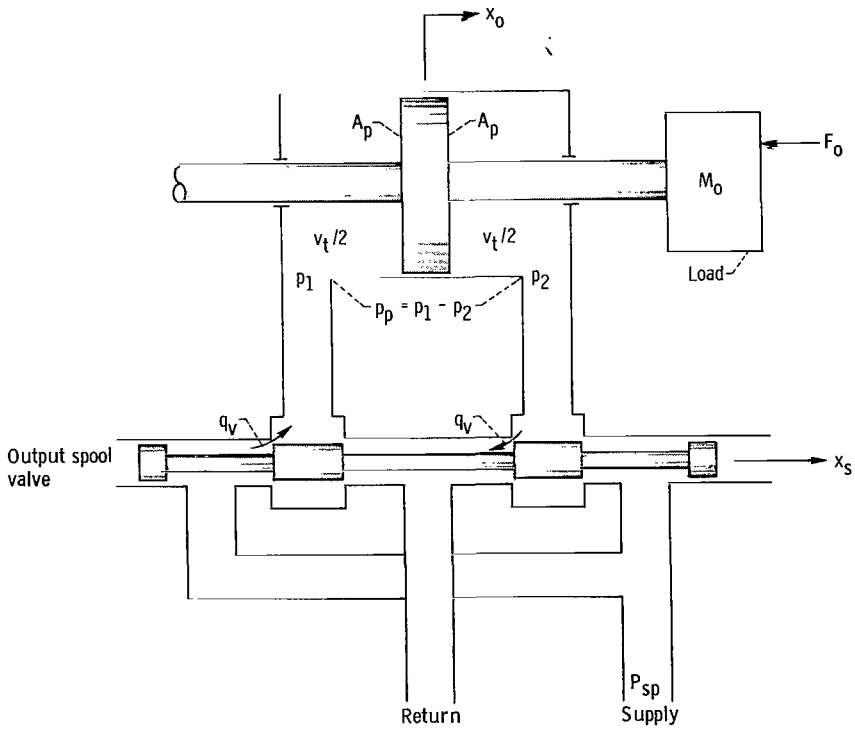

Figure 2. - Schematic representation of servovalve output, piston actuator, and load.

Servovalve Output and Actuator Coupling

It is also assumed that the servovalve and piston actuator will be hydraulically close-coupled. Therefore, the transmission line transport lag of the small connection length involved can be neglected. There will, however, be some amount of entrapped fluid which must be included to provide continuity to the describing equations. For the systems considered, the resonant frequency of the equivalent output mass M_o and this small volume of compressible fluid will occur at frequencies well beyond the range of interest (150 to 200 Hz). Thus, this resonance will not be a limiting factor to system dynamic performance.

The equation describing the interconnection of the servovalve and actuator is as follows:

$$\dot{x}_o A_p + \frac{V_t}{4\beta} \dot{p}_p = q_v \tag{3}$$

Equation (3) assumes that the piston is at mid-position and that the loads are such that the volumetric flows through each of the spool orifices are equal.

Two-Stage Servovalve

For high performance servosystems of the type being discussed in this report, a two-stage hydraulic servovalve is employed in almost all cases. This device is shown in detail in figure 3. It employs a spool valve output stage driven by a double jet flapper valve hydraulic preamplifier. This sensitive flapper is driven by the armature of an electromagnetic torque motor. In addition, a force feedback path from the spool to the torque motor armature is included to provide insensitivity to different operating modes. Reference 1 derives the basic relations which describe the operation of this control component. The final describing equations and the assumptions upon which they are based will now be presented.

The servovalve output is supplied as pressure and flow through the spool valve orifices (fig. 2) and through the control lines to the piston actuator. The equation which describes this output as a function of spool displacement x_s is defined by

$$q_v = C_s x_s \sqrt{p_v} \tag{4}$$

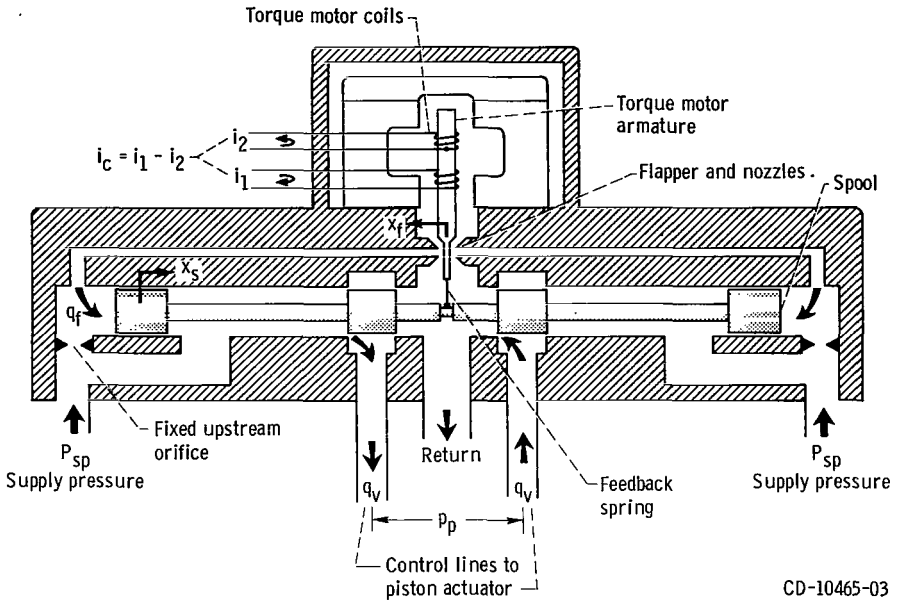

Figure 3. - Schematic representation of two-stage electrohydraulic servovalve.

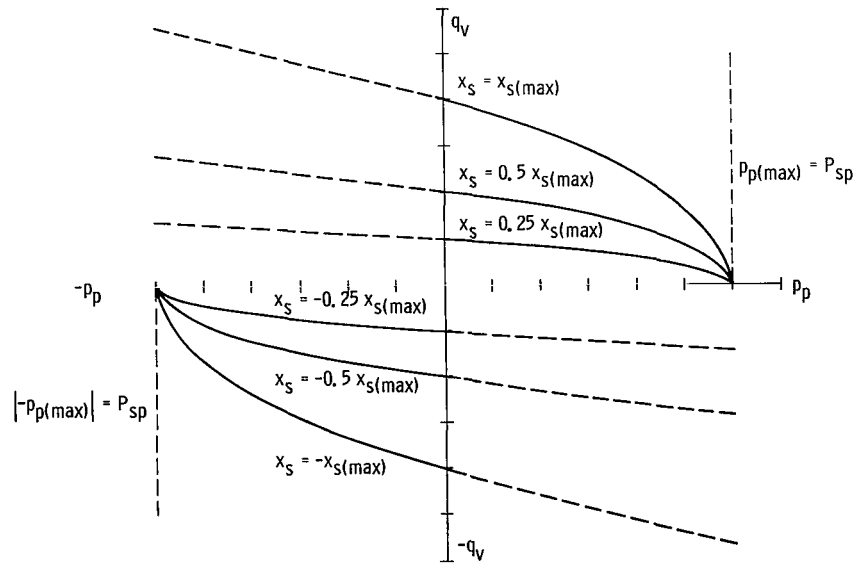

Figure 4. - Generalized servovalve output characteristics.

where

$$p_v = P_{sp} - p_p \tag{5}$$

and the return pressure is zero.

Figure 4 shows the family of valve output characteristics which result from this relation. From this figure, it can be seen that the nonlinear relation between output pressure and flow is physically limited by the maximum spool travel $x_{s(max)}$.

The spool displacement is determined by the action of the flapper valve preamplifier. In a well designed servovalve, the pressure forces required to accelerate the spool can be neglected. Thus, the spool motion will be dependent only on the flapper valve volumetric flow to the spool ends. This action is defined as follows:

$$x_s = \frac{1}{A_s} \int q_f \, dt \tag{6}$$

The double jet flapper valve which performs the hydraulic preamplification is a somewhat analytically complicated device. Reference 1, however, has investigated this device thoroughly. Using the results of this work, the flow to the spool from the flapper can be adequately approximated by the following linear relation:

$$q_f = K_{fn} x_f \tag{7}$$

Even though this simple relation is based on many assumptions, previous work in this area (ref. 2) has shown it to be quite valid in well designed high performance servovalves.

The flapper armature motion results from the effective torque applied to the torque motor armature. This torque is defined as follows:

$$T_{diff} = K_i i_c - K_w x_s \tag{8}$$

The armature consists of elements which form a spring/mass/damper system. Accordingly, it is represented by the following second order differential equation (ref. 2):

$$T_{diff} = \ddot{x}_f \frac{K_{fs}}{(\omega_{nf})^2} + \dot{x}_f \frac{(2\delta K_{fs})}{\omega_{nf}} + x_f K_{fs} \tag{9}$$

In addition to the physical limitation in the servovalve output stage capabilities caused by the maximum spool displacement, there is a limitation in the preamplifier flow as a result of the limit of flapper displacement $\pm x_{f(max)}$.

Torque Motor Current and Servoamplifier Output

The basic equation for a conventional voltage source output (low output impedance) amplifier driving inductive torque motor coils is defined by equation (10).

$$v_a = L_c \dot{i}_c + R_c i_c \tag{10}$$

The inherent inductive time constant L_c/R_c of the torque-motor coils is quite large. Several response improving techniques, however, are available. A precision servoamplifier, which has a high impedance output, has been developed (ref. 3) to accomplish this improvement. It has been employed experimentally in the type of fast response systems being discussed in this report. A detailed block diagram of this device with its associated nonlinear limitations is included as part of the complete nonlinear system block diagram of figure 5.

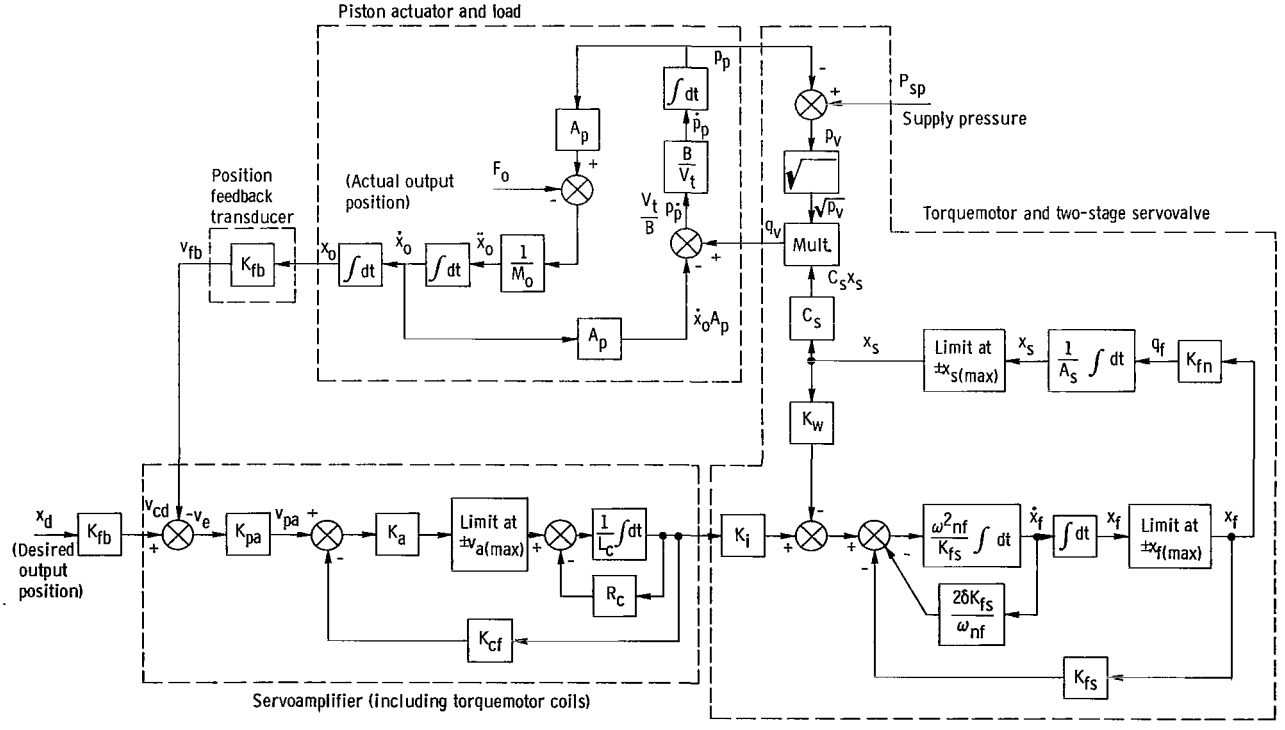

Figure 5. - Nonlinear block diagram representation of valve controlled piston servo system.

Feedback Monitoring, Signal Comparison, and Preamplification

To provide an indication of the output position of the actuator and load for feedback purposes, a position transducer has been employed. It can be represented analytically by the following equation.

$$K_{fb}x_o = v_{fb} \tag{11}$$

The comparison (summing) of the desired position x_d with the actual load position x_o takes place in the servoamplifier preamplifier input (fig. 5). It is defined by the following equations:

$$K_{fb}x_d = v_{cd} \tag{12}$$

$$v_{cd} - v_{fb} = v_e \tag{13}$$

The result of the above signal comparison v_e is amplified in the servoamplifier preamplifier stage. This operation is defined by equation (14).

$$K_{pa}v_e = v_{pa} \tag{14}$$

Nonlinear Block Diagram

The preceding equations can be combined to form the nonlinear block diagram of figure 5. Also included on the diagram are the physical component limitations. This nonlinear model can be used for analytical performance investigations of these fast response applications.

DYNAMIC PERFORMANCE RESULTS

Simulated Model Performance

The nonlinear dynamic model was used to determine the dynamic performance of a specific system configuration. The physical constants for this system are contained in table I. These specifications represent an actual servo actuator developed at Lewis Research Center. The actuator manipulates a variable area orifice to throttle fuel flows

TABLE I. - FUEL VALVE SERVO SYSTEM PHYSICAL CONSTANTS

Position scale factor (feedback transducer and input), K_{fb}, V/in. (V/cm)	80 (31.5)
Servoamplifier preamplifier gain, K_{pa}, V/V	0.46
Servoamplifier output forward loop gain, K_a, V/V	50
Servoamplifier output current feedback gain, K_{cf}, V/A	188
Torquemotor coil self-inductance, L_c, H	0.57
Torquemotor coil and servoamplifier equivalent resistance, R_c, Ohms	600
Torquemotor gain, K_i, in.-lbf/A (cm-N/A)	10 (114)
Torquemotor armature/flapper natural frequency, ω_{nf}, rad/sec	730 (2π)
Torquemotor armature/flapper damping ratio, δ, dimensionless	0.4
Stiffness of armature flapper, K_{fs}, in.-lbf/in. (cm-N/cm)	93 (414)
Flapper valve linear flow coefficient, K_{fn}, $(in.^3/sec)/in.$ $((cm^3/sec)/cm)$	150 (968)
Feedback wire stiffness, K_w, in.-lbf/in. (cm-N/cm)	13.5 (60.0)
Spool end area, A_s, $in.^2$ (cm^2)	0.026 (0.1677)
Piston area, A_p, $in.^2$ (cm^2)	0.25 (1.612)
Spool valve orifice flow coefficient, C_s, $(in.^3/sec)/\sqrt{lbf}$ $((cm^3/sec)/\sqrt{N})$	32.5 (251.5)
Hydraulic supply pressure, P_{sp}, $lbf/in.^2$ (N/cm^2)	3000 (2070)
Equivalent actuator and output load mass, M_o, $lbf\text{-}sec^2/in.$ $(N\text{-}sec^2/cm)$	0.00155 (0.00271)
Maximum servoamplifier output voltage, $v_{a(max)}$, V	±15
Maximum flapper armature displacement, $x_{f(max)}$, in. (cm)	±0.0012 (±0.00305)
Maximum spool displacement, $x_{s(max)}$, in. (cm)	±0.015 (±0.0381)
Rated servovalve flow, Q_r, $in.^3/sec$ (cm^3/sec)	15.4 (252.5)
Optimum piston area, A_p^*, $in.^2$ (cm^2)	0.0744 (0.480)
Spool valve linear flow coefficient, K_s, $(in.^3/sec)/in.$ $((cm^3/sec)/cm)$	1030 (6640)

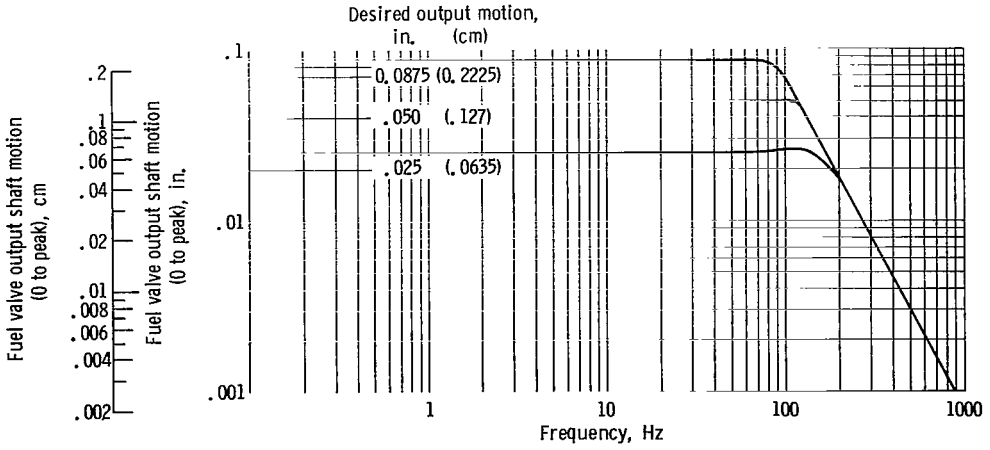

Figure 6. - Model dynamic performance - simulated fuel valve servo.

at high rates of response for turbojet engine dynamics studies. The evaluation was performed by simulating the model on an analog computer. The dynamic performance (frequency response) for various levels of desired output shaft motion is shown in figure 6.

Experimental Performance

The actual experimental dynamic performance exhibited by the system described by table I is shown in figure 7. For comparison purposes, the simulated model performance has been included in this figure. The correlation between the two sets of curves demonstrates the accuracy of the analytical nonlinear model.

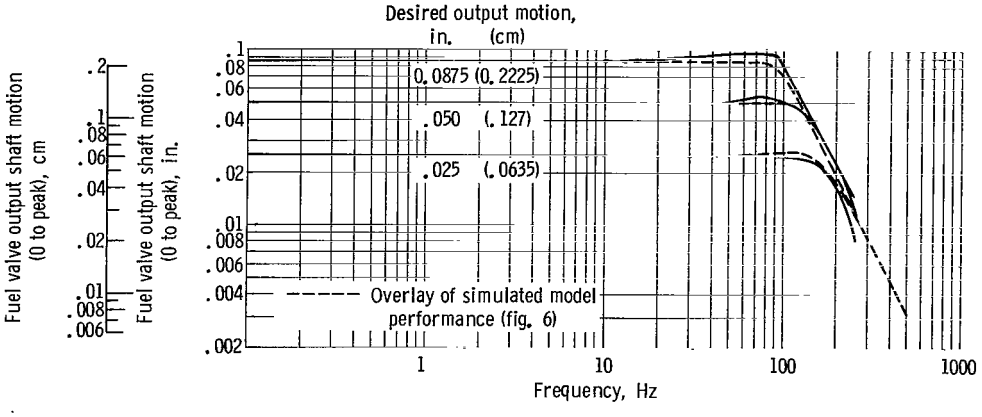

Figure 7. - Experimental dynamic performance - fuel valve servo.

DISCUSSION OF PERFORMANCE LIMITATIONS

It can be seen from the curves of figures 6 and 7 that, for a desired output shaft motion, the actual sinusoidal motion is attenuated at higher frequencies. In addition, the attenuation occurs at lower frequencies as the magnitude of desired output motion increases. Thus, some limiting phenomenon is taking place in the actuation system. In predicting the limitation to unattenuated sinusoidal output motion of a high performance electrohydraulic servo, conventional practice defines two limit criteria. These are velocity (flow) and acceleration (pressure) limits imposed by the output capacity of the servovalve selected for the application.

Figure 4 shows that the maximum output capabilities occur along the $x_{s(max)}$ characteristic. The power transferred to the load for various points (on this output characteristic) has a maximum value at some specific point. The derivation of the peak power

transfer point is considered in reference 1; and, therefore, only the results will be included here. At peak power, pressure and flow are defined by equations (15) and (16).

$$p_{p(pp)} = \frac{2}{3} P_{sp} \tag{15}$$

$$q_{v(pp)} = C_s x_{s(max)} \sqrt{\frac{1}{3} P_{sp}} \tag{16}$$

Conventional servovalve terminology selects these values of pressure and flow to define acceleration (pressure) and velocity (flow) limit lines for the actuator output. Conventional practice also designates the flow defined by equation (16) as the servovalve rated flow Q_r. Selection of the pressure and flow of equations (15) and (16) defines the cross-hatched region of figure 8. For practical purposes, therefore, sinusoidal output motion is conservatively restricted to pressures and flows which do not exceed this region. Using these limiting values of pressure and flow, the equations for the conventionally accepted acceleration (pressure) and velocity (flow) limit lines can now be derived.

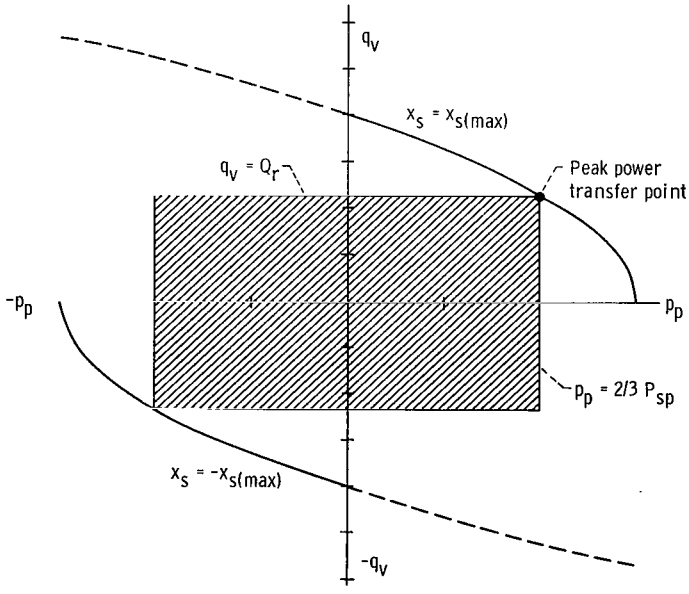

Figure 8. - Region of unlimited dynamic performance using peak power transfer criteria.

Velocity (Flow) Limit Criterion

If the output piston position x_o varies sinusoidally, the following equations can be written:

$$x_o = X_o \sin \omega t \tag{17}$$

$$\dot{x}_o = X_o \omega \cos \omega t \tag{18}$$

Equation (3) which defines the servovalve output flow to the load is repeated for convenience.

$$q_v = A_p \dot{x}_o + \frac{V_t}{4\beta} \dot{p}_p \tag{3}$$

Since the entrapped volume is being considered small, the second term on the right side of equation (3) can be neglected. This results in

$$q_v = A_p \dot{x}_o \tag{19}$$

Combining equations (19) and (17) yield

$$\frac{q_v}{A_p} = X_o \omega \cos \omega t \tag{20}$$

Evaluating only the peak value of the parameters yields the following velocity limit relation:

$$\frac{Q_r}{A_p} = X_o \omega \tag{21}$$

Acceleration (Pressure) Limit Criterion

The output acceleration under sinusoidal motion is defined as

$$\ddot{x}_o = -X_o \omega^2 \sin \omega t \tag{22}$$

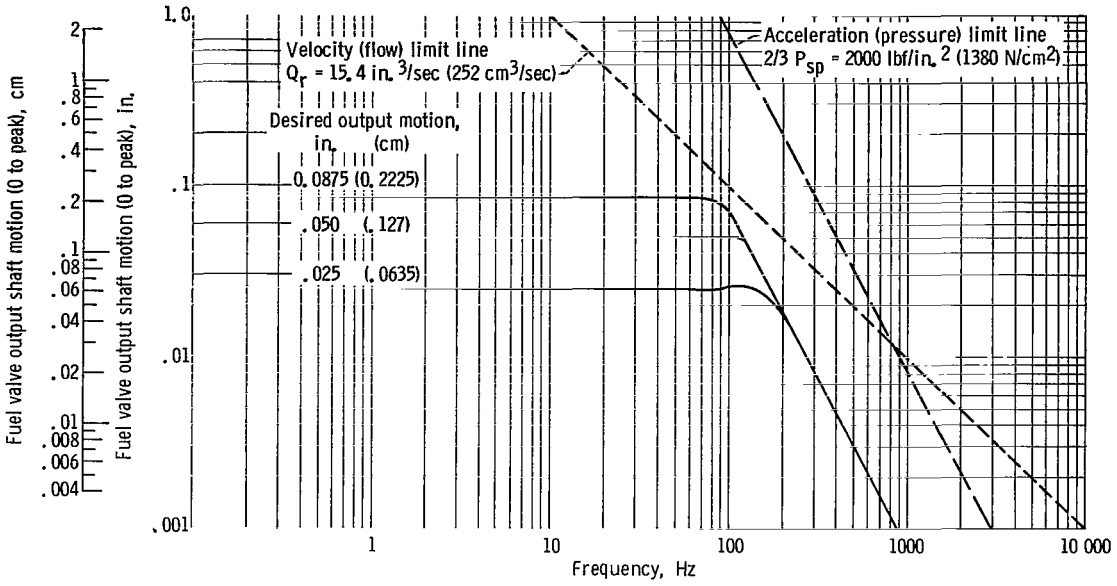

Figure 9. - Fuel valve analytical model performance with velocity and acceleration limits.

By making the assumption of only a pure mass load on the actuator, the following equation results:

$$p_p A_p = M_o \ddot{x}_o \tag{23}$$

Thus, substituting equations (22) and (15) into equation (23) and considering only peak values, the following acceleration limit relation results:

$$\frac{2}{3} P_{sp} \frac{A_p}{M_o} = X_o \omega^2 \tag{24}$$

Using the specifications for the fuel valve servo (table I), the velocity and acceleration limit curves can be added to the data of figure 6. This composite is shown in figure 9. Since the system attenuation occurs well below these limits, it is evident that some other factor has limited the response.

Flapper Limit Criterion

It has been found both from observations made on the simulation of the nonlinear model and by analytical derivation that this limit is caused by the internal flow limitation

within the servovalve hydraulic preamplifier. In other words, the maximum flow to the servovalve output stage (spool valve) is not sufficient to permit it to slew (travel at maximum velocity) fast enough to supply rated flow Q_r at the higher frequencies. This phenomenon does not normally arise in lower response applications.

It should be pointed out that the high frequency (high flow) limitation of two-stage servovalves is inherent in well designed versions of these devices. Stability of jet-flapper valve elements designed for reliable long-term performance imposes certain limits on the orifice sizing and clearances, and thus on flapper flow. A detailed discussion of these facts appears in reference 1.

As a result of the preceding observations, the flapper stage flow limitation must be used as a third criterion for predicting the maximum attainable dynamic performance of high performance electrohydraulic servo systems. The derivation of this criterion is as follows:

When the servovalve output is limited to a region bounded by the pressure and flow at maximum power transfer (fig. 8), the nonlinear relation of equation (4),

$$q_v = C_s x_s \sqrt{p_v} \tag{4}$$

can be adequately approximated by

$$q_v = K_s x_s \tag{25}$$

where

$$K_s = \left.\frac{\partial q_v}{\partial x_s}\right|_{p_v = 1/3 P_{sp}}$$

Substituting this linearized relation for the valve output flow q_v into equation (19) results in

$$K_s x_s = A_p \dot{x}_o \tag{26}$$

Substituting equation (18) into equation (26) and rearranging result in

$$x_s = \frac{A_p X_o}{K_s} \omega \cos \omega t \tag{27}$$

Differentiating yield

$$\dot{x}_s = -\frac{A_p}{K_s}\omega^2 X_o \sin \omega t \tag{28}$$

Differentiating equation (6) and rearranging results in

$$q_f = A_s \dot{x}_s \tag{29}$$

Equation (7) is repeated for convenience.

$$q_f = K_{fn} x_f \tag{7}$$

Combining equations (28), (29), and (7) and considering only peak values of sinusoidal motion results in the following equation:

$$\frac{A_p \omega^2 X_o}{K_s} = \frac{K_{fn} x_{f(max)}}{A_s} \tag{30}$$

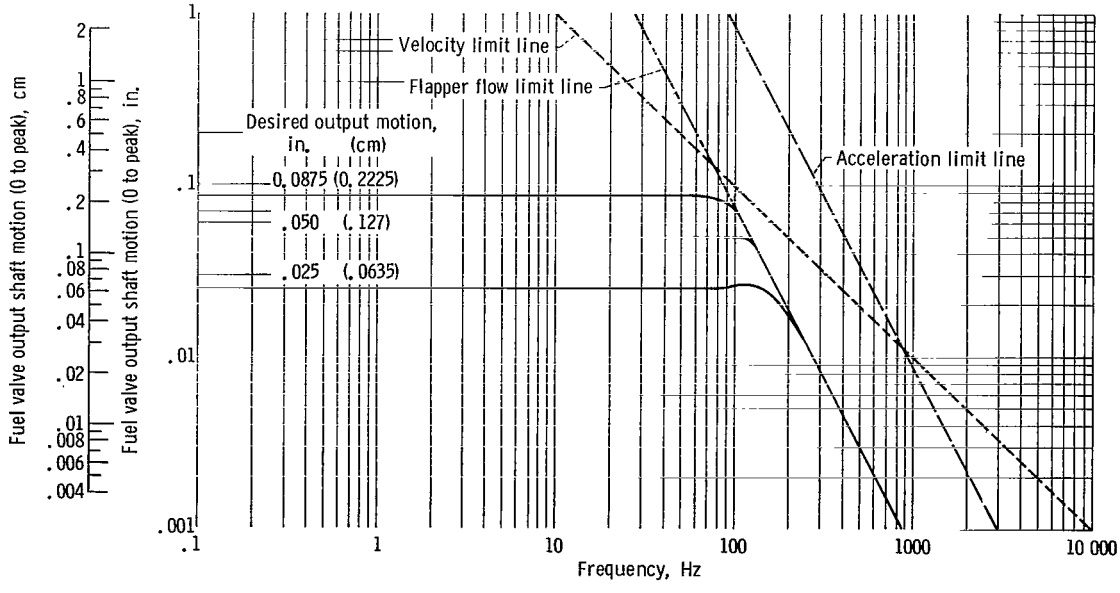

Figure 10. - Fuel valve performance with velocity, acceleration, and flapper flow limits.

Rearranging equation (30) results in the following flapper flow limit relation

$$X_o\omega^2 = \frac{K_{fn}K_s x_{f(max)}}{A_p A_s} \tag{31}$$

Using the specifications for the previous example (table I), this limiting criterion can be combined with the composite curves of figure 9 to generate figure 10. The close correlation of this new limit with the actual system maximum dynamic performance demonstrates the validity of this criterion and emphasizes its necessity for performance prediction purposes in fast response (150 to 200 Hz) applications.

GENERALIZED DESIGN CRITERIA FOR REGION OF MAXIMUM DYNAMIC PERFORMANCE CAPABILITY

The three limiting relations defined by equations (21), (24), and (31) are repeated here for clarity.

Velocity limit

$$X_o\omega = \frac{Q_r}{A_p} \tag{21}$$

Acceleration limit

$$X_o\omega^2 = \frac{\frac{2}{3}P_{sp}A_p}{M_o} \tag{24}$$

Flapper flow limit

$$X_o\omega^2 = \frac{K_{fn}K_s x_{f(max)}}{A_p A_s} \tag{31}$$

For a specific application in which the load mass and the supply pressure available are specified, these criteria are all a function of the piston actuator area and the capacity of specific servovalves. For a particular servovalve, the curves will depend only on piston area. Figure 11 is presented to show the generalized displacement or shift of

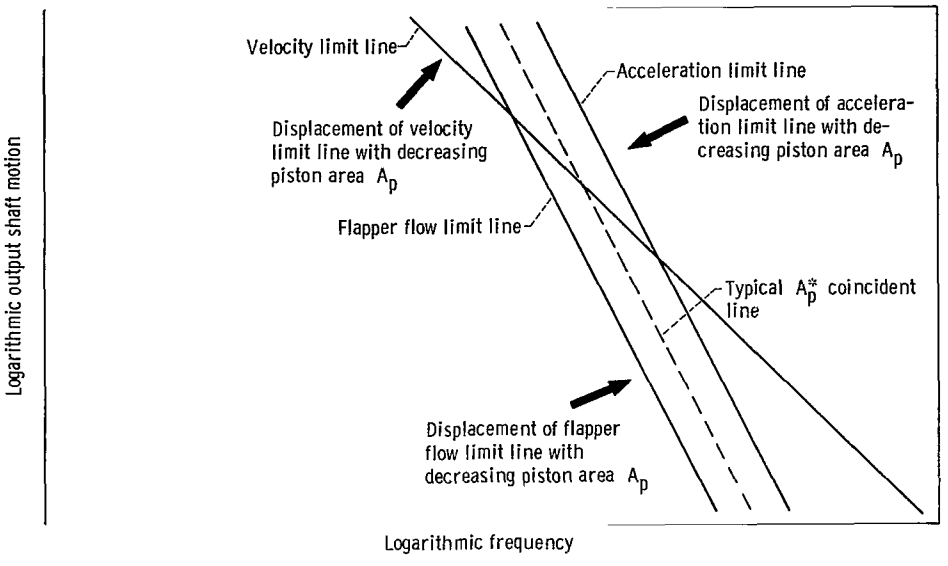

Figure 11. - General limit lines - dependence on piston area.

each limit line as a function of piston area. It can be seen from this figure that for a specific value of piston area A_p the parallel flapper flow line and output acceleration line can be made to coincide. The piston area at which this concidence occurs can be determined as follows:

Equating equations (24) and (31) yields

$$\frac{K_{fn}K_s x_{f(max)}}{A_s A_p} = \frac{\frac{2}{3}P_{sp}A_p}{M_o} \tag{32}$$

Solving for the coincident piston area yields

$$A_p^* = \sqrt{\frac{x_{f(max)}M_o K_{fn}K_s}{\left(\frac{2}{3}\right)(A_s)(P_{sp})}} \tag{33}$$

Using the "optimum" piston area A_p^* for the fuel valve system specified in table I will maximize the high frequency region of dynamic performance capability. This region is shown cross-hatched in figure 12. The dashed curve on this figure is the boundary of the dynamic performance capabilities of the experimental fuel valve system. This system used an area greater than A_p^*. The figure shows that selection of a "nonoptimum" area

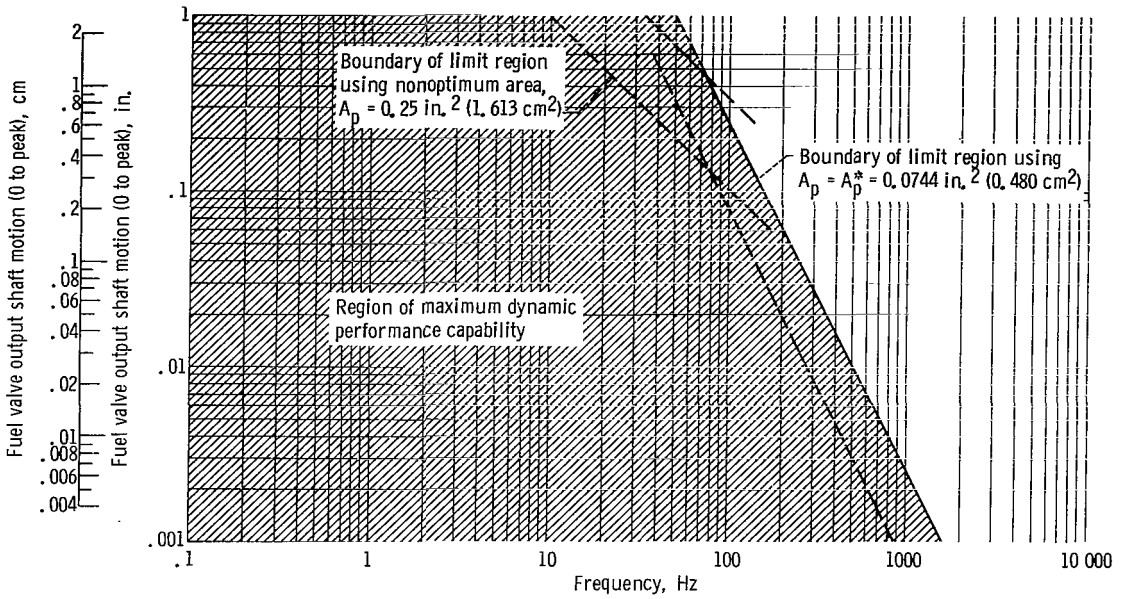

Figure 12. - Optimized dynamic performance capability region.

results in less than maximum performance capabilities.

It should be pointed out that the piston area ($A_p^* = 0.0744$ in.^{2} or 0.480 cm^2), which results from equation (33) is relatively small. If opposing loads other than pure mass are present, the adequacy of this area must be examined carefully. There are many actuation applications, however, where the area selected by equation (33) will permit successful operation throughout the entire region of dynamic performance capability.

FURTHER EXTENSIONS OF THE GENERALIZED LIMIT CRITERIA

Figure 12 shows that the boundary of dynamic performance capabilities consists of two straight lines which intersect at a common point. For the optimized piston area case, they are the piston velocity and coincident flapper flow and piston acceleration limit lines. It should be noted that the piston velocity limit line has a slope of -1 on the logarithmic plot while the flapper flow or piston acceleration limit lines have a slope of -2. The intersection point or "corner point" from which these lines emanate has associated with it displacement and frequency coordinates which will be defined as x_o^{**} and ω^{**}, respectively.

Noting again the direction of the flapper flow limit line shown on figure 11 for decreasing piston area (to the right), it can be seen that the corner point (x_o^{**}, ω^{**}) for all piston areas greater than or equal to A_p^* will be determined by the intersection of the

piston velocity and flapper flow limit lines. The relation for these coordinates can be determined as follows:

Substituting equation (21) into equation (31) and solving for ω^{**} results in equation (34).

$$\omega^{**} = \frac{K_{fn}K_s x_{f(max)}}{A_s Q_r} \tag{34}$$

for $A_p \geq A_p^*$. Substituting this expression for ω^{**} into equation (21) and solving for x_o^{**} yields the following relation:

$$x_o^{**} = \frac{(Q_r)^2 A_s}{K_{fn}K_s x_{f(max)} A_p} \tag{35}$$

for $A_p \geq A_p^*$.

For piston areas smaller than A_p^*, a review of figure 11 will show that the piston acceleration limit line will lie to the left of the flapper flow limit line. Thus, for the case $A_p < A_p^*$ the point of intersection (x_o^{**}, ω^{**}) for the boundary of dynamic performance capability will be determined by the conventional piston acceleration and velocity limit lines. Relations for the coordinates x_o^{**} and ω^{**} can be determined as follows:

Substituting equation (21) into equation (24) and solving for ω^{**} yields

$$\omega^{**} = \frac{\frac{2}{3} P_{sp} A_p^2}{Q_r M_o} \tag{36}$$

for $A_p < A_p^*$. Substituting equation (36) into equation (21) and solving for x_o^{**} yields the following relation:

$$x_o^{**} = \frac{(Q_r)^2 M_o}{(A_p^3)\left(\frac{2}{3} P_{sp}\right)} \tag{37}$$

for $A_p < A_p^*$.

Figure 13 shows the locus of the point of intersection (x_o^{**}, ω^{**}) for various piston areas. The coordinates have been normalized to the point of intersection at the optimum area A_p^*.

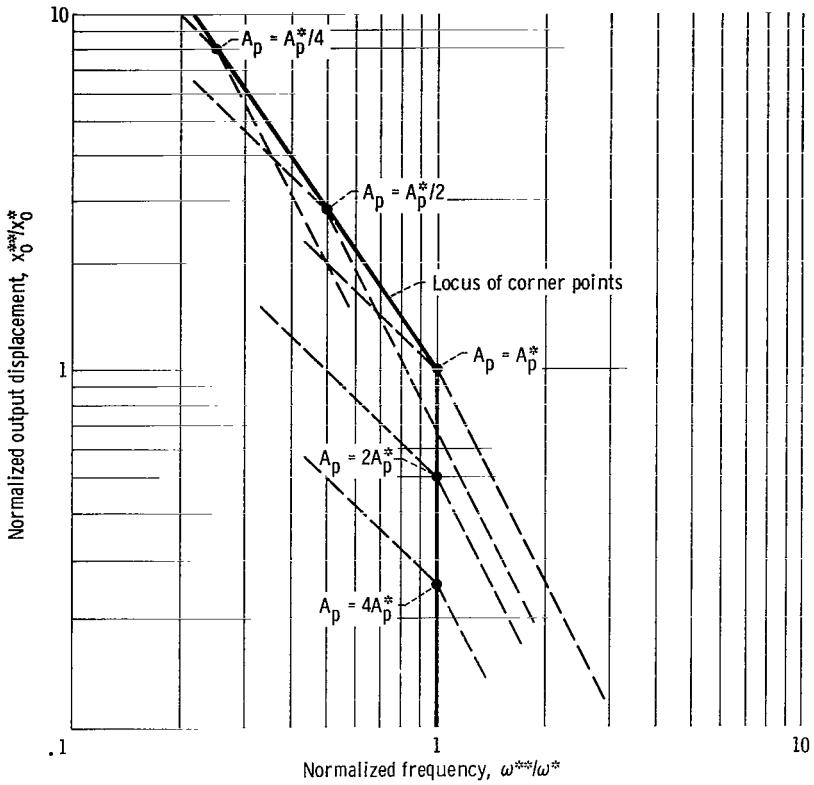

Figure 13. - Locus of normalized corner points for region of dynamic performance capabilities.

The locus for piston areas greater than A_p^* is determined by equations (34) and (35). Since the frequency ω^{**} defined by equation (34) is not a function of the piston area A_p, the locus for $A_p > A_p^*$ is the vertical line shown in figure 13.

If the piston area A_p is less than the optimum area A_p^*, the locus may be determined from equations (36) and (37). These two equations imply that

$$x_o^{**} \alpha \omega^{-3/2}$$

for $A_p < A_p^*$. Hence, the locus of figure 13 has a slope of -3/2 for $A_p < A_p^*$.

Knowledge of the coordinates at $A_p = A_p^*$ therefore is sufficient to completely determine the corner point locus. For this reason, the locus of figure 13 has been normalized to the coordinates at this point. The coordinates at $A_p = A_p^*(x_o^*, \omega^*)$ are defined by

$$x_o^* = \frac{(Q_r)^2 \cdot A_s}{K_{fn} \cdot K_s x_{f(max)} \cdot A_p^*} \tag{38}$$

$$\omega^* = \frac{K_{fn} \cdot K_s \cdot x_{f(max)}}{A_s \cdot Q_r} \tag{39}$$

where

$$A_p^* = \sqrt{\frac{x_{f(max)} \cdot M_o \cdot K_{fn} \cdot K_s}{\left(\frac{2}{3}\right)(A_s)(P_{sp})}} \tag{33}$$

The ratio of piston areas (A_p/A_p^*) determines where the corner point is on the normalized locus of figure 13. From equations (36), (37), and (38), the following relations can be derived:

For $A_p > A_p^*$

$$\frac{x_o^{**}}{x_o^*} = \frac{A_p^*}{A_p} < 1 \tag{40}$$

For $A_p < A_p^*$

$$\frac{x_o^{**}}{x_o^*} = \left(\frac{A_p^*}{A_p}\right)^3 > 1 \tag{41}$$

and

$$\frac{\omega^{**}}{\omega^*} = \left(\frac{A_p}{A_p^*}\right)^2 < 1 \tag{42}$$

Thus, equations (33) and (38) through (42) completely describe the position of the corner point. On the normalized plot of figure 13 also are included several boundary lines which emanate from the corner points. The velocity limit has a slope of -1 to the left, and the flapper flow or acceleration limits have a slope of -2 to the right.

With this rather complete picture of the possible regions of dynamic performance capability, a few observations should be made. For piston areas greater than the optimum A_p^*, the boundary lines move to the left actually decreasing the region of dynamic performance capability. Thus, unless the requirements of the opposing force loads

demand the larger piston areas, A_p^* will result in the highest frequency-amplitude performance.

For piston areas smaller than A_p^*, figure 13 shows that high frequency performance is sacrificed to gain lower frequency operation at larger amplitudes of x_o.

CONCLUDING REMARKS

A detailed analysis has been made of the nonlinear aspects of electrohydraulic valve-controlled piston servo actuation systems for high response (150 to 200 Hz) research applications. The analysis has considered the major load to be inertial (mass) and has assumed the actuator to be close-coupled to the valve. The analysis has shown that under these conditions, an internal servovalve limitation (flapper flow limitation) previously considered insignificant greatly influences the dynamic performance capabilities of fast response systems. This limitation has been investigated and formulated into general design criteria. These criteria will define a maximum region of dynamic performance capability for a particular system. Classical control techniques can then be employed to insure stable dynamic performance throughout this region of capability.

Lewis Research Center,
National Aeronautics and Space Administration,
Cleveland, Ohio, June 17, 1969,
720-03-00-69-22.

APPENDIX - SYMBOLS

A	area, $in.^2$ (cm^2)
C	coefficient (nonlinear)
F	force, lbf (N)
i	current (instantaneous), A
K	scale factor or linearized coefficient
L	self-inductance, H
M	mass, $lbf\text{-}sec^2/in.$ ($N\text{-}sec^2/cm$)
P	pressure (steady-state), $lbf/in.^2$ (N/cm^2)
p	pressure (instantaneous), $lbf/in.^2$ (N/cm^2)
Q	volumetric flow (steady-state), $in.^3/sec$ (cm^3/sec)
q	volumetric flow (instantaneous), $in.^3/sec$ (cm^3/sec)
R	resistance, ohms
T	torque, in.-lbf (cm-N)
t	time, sec
V	volume, $in.^3$ (cm^3)
v	voltage (instantaneous), V
X	linear displacement (peak of sine wave), in. (cm)
x	linear displacement (instantaneous), in. (cm)
β	bulk modulus, $lbf/in.^2$ (N/cm^2)
δ	damping ratio (dimensionless)
π	numerical constant - 3.1416
ρ	mass density, $lbf\text{-}sec^2/in.^4$ ($N\text{-}sec^2/cm^4$)
ω	frequency, rad/sec

Subscripts:

a	amplifier
c	coil
cd	command
cf	current feedback
d	demand
diff	difference
e	error
f	flapper
fb	feedback
fn	flapper nozzle
fs	flapper spring
i	current
max	maximum
nf	natural frequency
o	output
p	piston
pa	preamplifier
pp	peak power
r	rated
s	spool
sp	supply pressure
t	total

v valve

w wire

Superscripts:

* optimum

** corner point designation

. first derivative with respect to time

.. second derivative with respect to time

REFERENCES

1. Merritt, Herbert E.: Hydraulic Control Systems. John Wiley & Sons, Inc., 1967.
2. Thayer, W. J.: Transfer Functions for Moog Servovalves. Tech. Bull. #103, Moog Servocontrols, Inc.
3. Zeller, John R.: Design and Analysis of a Modular Servoamplifier for Fast-Response Electrohydraulic Control Systems. NASA TN D-4898, 1968.

"The aeronautical and space activities of the United States shall be conducted so as to contribute . . . to the expansion of human knowledge of phenomena in the atmosphere and space. The Administration shall provide for the widest practicable and appropriate dissemination of information concerning its activities and the results thereof."

—NATIONAL AERONAUTICS AND SPACE ACT OF 1958

NASA SCIENTIFIC AND TECHNICAL PUBLICATIONS

TECHNICAL REPORTS: Scientific and technical information considered important, complete, and a lasting contribution to existing knowledge.

TECHNICAL NOTES: Information less broad in scope but nevertheless of importance as a contribution to existing knowledge.

TECHNICAL MEMORANDUMS: Information receiving limited distribution because of preliminary data, security classification, or other reasons.

CONTRACTOR REPORTS: Scientific and technical information generated under a NASA contract or grant and considered an important contribution to existing knowledge.

TECHNICAL TRANSLATIONS: Information published in a foreign language considered to merit NASA distribution in English.

SPECIAL PUBLICATIONS: Information derived from or of value to NASA activities. Publications include conference proceedings, monographs, data compilations, handbooks, sourcebooks, and special bibliographies.

TECHNOLOGY UTILIZATION PUBLICATIONS: Information on technology used by NASA that may be of particular interest in commercial and other non-aerospace applications. Publications include Tech Briefs, Technology Utilization Reports and Notes, and Technology Surveys.

Details on the availability of these publications may be obtained from:

SCIENTIFIC AND TECHNICAL INFORMATION DIVISION

NATIONAL AERONAUTICS AND SPACE ADMINISTRATION

Washington, D.C. 20546